THE BELL SYSTEM TECHNICAL JOURNAL
Vol. 60, No. 7, September 1981
Printed in U.S.A.

Profile Characterization of Optical Fibers—A Comparative Study

By H. M. PRESBY

(Manuscript received February 12, 1981)

The refractive index profiles of several multimode optical fibers were measured by four of the current state-of-the-art techniques. These include interference microscopy on slab samples, transverse interference microscopy on whole fiber samples, the focusing method, and the refracted near-field method. The profile of the parent preform of one of the fibers was also measured by both the focusing method and by a ray-tracing approach. Comparisons of the results and the measurement methods are made emphasizing the applicability and use of the various techniques.

I. INTRODUCTION

Precise methods for measuring index profiles in both multimode and single-mode optical fibers and preforms are required if the desired ideal index distributions are to be produced. This paper will provide a comparison of four current state-of-the-art techniques for making these measurements on fibers and two similarly current methods used for preforms. Implications of the results especially related to the applicability and utilization of the various techniques will be discussed.

It is important to have some feeling for the structure of the object being profiled. The fibers and the preform studied were produced by the modified chemical vapor deposition process.[1] In this procedure a silica tube is mounted on a glass-working lathe and slowly rotated while reactants and dopants flow through it in an oxygen stream. An oxy-hydrogen burner is slowly traversed along the outside of the tube to provide simultaneous deposition and fusion of a layer of the reacting materials. On the order of 50 layers are deposited by multiple passes of the burner. To fabricate graded-index fibers, the dopant concentration is gradually increased with increasing layer number.

At the conclusion of deposition, the temperature of the burner is

raised to collapse the tube into a solid preform. A diagnostigram[2] of the remaining end of the preform after being pulled into a fiber is shown in Fig. 1a. This display is obtained by expanding and collimating the light from a CW laser and allowing it to impinge upon the preform. The diagnostigram provides a simple and rapid nondestructive means of investigating internal layer structure. Details of its operation can be found in the Appendix. A shadow of the blunted end of the preform is seen at the lower right and each of the deposition layers is seen as a horizontal line. The uppermost bright line is the core-cladding boundary and the region immediately below it is a 320-μm-thick barrier layer. The core radius is about 3.5 mm and the length of preform seen in the diagnostigram is 12 cm. The point to note is the rich structure and resolvability of the deposition layers. Another view of this structure can be obtained by immersing the preform in index-matching oil and observing the incoherently illuminated core with a video camera, as is done in the focusing method.[3] This representation, shown in Fig. 1b for a several millimeter length of preform, also emphasizes the individual layer structure, which is in addition displayed by the curve at the side of the display.

These structural variations also appear, appropriately scaled, in the fiber in a one-to-one correspondence[4] and corroborates the fact that the same distribution of refractive index that is introduced into the preform exists in the fiber.[5] Generally, the scale of the variations in the fiber is on the order of less than a wavelength and they are, therefore, not observed by the measurement technique. Notable exceptions occur near the axis where the deposition layers are thickest and in any region where either several layers have the same index or thicker than normal layers are produced, due to fabrication faults.

The profile, built up by varying the dopant concentration in each of the layers, can be measured by a variety of techniques. How accurately the measurements should be made and which technique is best for making them are always difficult questions to answer since they involve trade-offs of many factors. To be included are time, cost, and effort considerations, all of which one would like to minimize, and sensitivity, accuracy, and resolution which one would like to maximize.

A handle on the question of accuracy is provided by the following considerations. The theoretical bandwidth that can be realized with an optimum profile is about 8000 MHz $\times$ km for a fiber with a maximum index difference value of 0.02.[6] To achieve this high bandwidth requires that the exponent, g, of the power-law profile have a definite optimum value near $g = 2$ (for germanium dopant and an operating wavelength of 0.9 μm). A departure of only 0.05 from this optimum g value is sufficient to reduce the fiber bandwidth by more than one order of magnitude. Clearly the profiling technique must determine g to better than 0.05 if a meaningful correlation between

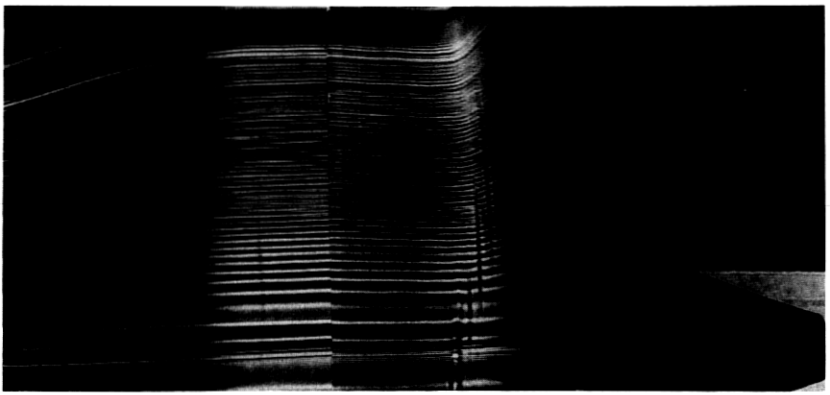

(a)

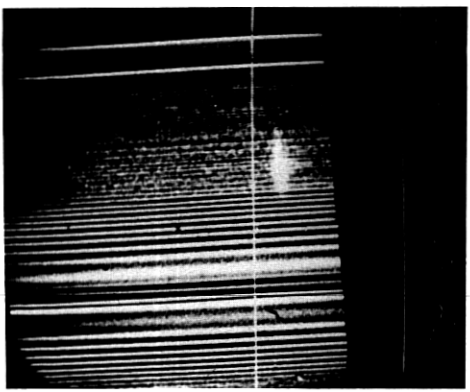

(b)

Fig. 1—Layer structure of MCVD fabricated preform as observed by: (a) diagnostrigram, and (b) index immersion.

fiber performance and index profile is to be obtained. In order to achieve this accuracy, $\Delta n(r)$ [the difference between the refractive index of the fiber core and its cladding value] must be measured with a precision of 1 part in 10^4.

Very slight local distortions of the refractive index profile from its optimum shape also decrease the fiber bandwidth markedly. A distortion of ten sinusoidal periods over the fiber radius with an rms amplitude of 0.6 percent of the maximum index difference reduces the bandwidth from 8000 MHz × km to about 200 MHz × km.[6] An rms distortion amplitude of only 0.15 percent for the same ripples reduces the bandwidth to about 800 MHz × km. The precision of the $\Delta n(r)$ measurement would again have to be about 1 part in 10^4 to detect even the 0.6 percent distortion. In addition, of course, the spatial resolution of the technique must be sufficient to resolve the perturbations.

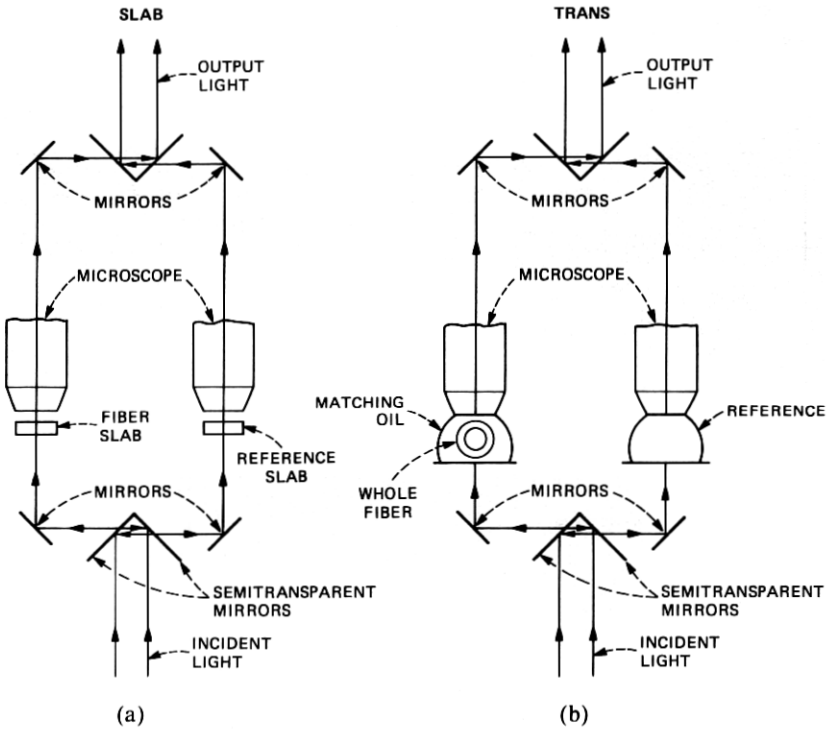

Fig. 2—Schematic diagram of (a) slab interferometric method, and (b) transverse interferometric method. The interference microscope used in both cases is identical.

II. PROFILE MEASUREMENT METHODS

The specific profiling methods used in this study are shown diagrammatically in Figs. 2 and 3. They are interference microscopy on SLAB samples (Fig. 2a); transverse interferometry on whole fiber samples (Fig. 2b); the focusing method (Fig. 3a); and the refracted near-field method (Fig. 3b). They are abbreviated by the terms SLAB, TRANS, FOCUS, and RNF, respectively. These methods will be discussed briefly; further details on their practical implementation can be found in the Appendix.

2.1 Slab interferometry

Interference microscopy on SLAB samples, utilizing the potential accuracy of interferometry was historically the first of these methods to be used,[7] and is generally accepted as the method to which newly developed techniques are compared. The SLAB sample is cut from an encapsulated fiber (or preform tip) and polished so that the faces are flat and parallel. The cutting and polishing procedures are both difficult and time-consuming. Special techniques are required to avoid

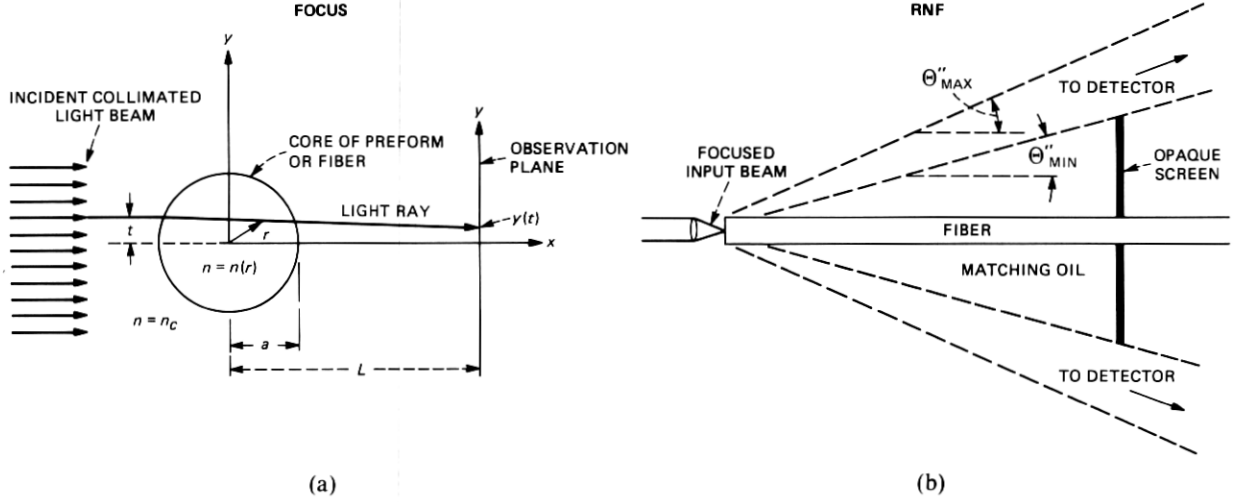

Fig. 3—Principle of operation of (a) focusing method, and (b) refracted near-field (RNF) technique.

composition-dependent thickness variations, which can lead to substantial errors.[8] It is also necessary for the sample to be thin enough so that rays traversing it are not bent and focused, producing curved wavefronts and, hence, erroneous results. Sample preparation requires about one day. This time can be reduced on a per-sample basis by processing several different fibers, which have been epoxied into one capillary tube, at the same time. It should also be noted that this procedure is not inherently nondestructive.

To observe the samples, of course, an interference microscope is required. Interference lens attachments to ordinary microscopes generally involve passing the light through the specimen twice, thus compounding possible errors. Best results are obtained with a single-pass Mach-Zehnder geometry, but microscope cost and availability are additional major considerations in adopting this method.

Relative index values accurate to about 2 parts in 10^4 can be realized routinely and by electronically processing the output of the microscope measurements relatively accurate to about 1 part in 10^5, as necessary, for example, in profile dispersion work, have been achieved.[9] Automatic computer processing of the output also serves to reduce analysis time. Spatial index resolution is somewhat limited in that it is not possible to combine maximum lateral resolution and exact phase measurements in a single instrument.[10]

2.2 Transverse interferometry

Sample preparation can be eliminated by using the transverse interferometric method (Fig. 2b). In this technique, a length of fiber is immersed in matching oil on the stage of the interference microscope and illuminated at right angles transverse to its axis. The matching oil removes the influence of the outer cladding boundary. The total optical path length of a light ray is expressed as an integral and the index distribution is obtained from the measured fringe shift by solving an integral equation.[11] Unlike the SLAB approach, in which the entire core is accessible, transverse interferometry assumes circular symmetry and, hence, geometry variations, which can adversely affect the profile, will not be detected unless special care is taken to make several measurements for different rotational positions of the fiber. By automating the measurement, index profiles of a fiber can be obtained within a few minutes after its manufacture. The accuracy of the method is about an order of magnitude less than that of the SLAB approach, and it is subject to a large error in the region near the fiber axis. On the other hand, this technique resolves detail in the fiber structure with higher resolution than the SLAB method, as will be seen later in the actual profiles.

2.3 Focusing method

The focusing method[12] (Fig. 3a) is similar to transverse interferometry in that it is also nondestructive and uses transverse illumination. Otherwise they are very different. The focusing method does not require an interference microscope or rely in any way on interferometry. Moreover, the technique is readily applicable with high accuracy to fiber preforms.[3]

In this method, the fiber, observed with a microscope and the preform with a camera lens, are immersed in index matching fluid. The core, acting as a cylindrical lens, focuses the light, whose power density distribution in the observation plane is detected by a video camera. After digitizing the power density a computer calculates the index profile by solving an integral equation. The profiles so obtained from circularly symmetric cores are comparable in accuracy and resolution to those produced by interference microscopy of SLAB samples.[13]

Extreme experimental care, however, is involved in the focusing method since it measures absolute light intensities. The optics, matching oil, and fiber (or preform) itself must be very clean; the video detector must be linearized and the incident light intensity must be uniform, either intrinsically or through a calibration procedure.

2.4 Ray tracing

A related method to measure the profile in preforms is ray tracing.[14] Further details of this technique are also given in the Appendix. This method involves scanning a focused laser beam perpendicular to the axis of the index-matched preform and recording the exit angle of the beam as a function of distance from the axis. The profile of the preform is then reconstructed by taking the inverse Abel transform of the deflection function. Indeed, the mathematics of this and the focusing method are nearly identical[12] and lead to very similar profiles, if an equal number of data points are measured and processed.

2.5 Refracted near-field

The refracted near-field (RNF) method[15] (Fig. 3b) relies on the power escaping sideways from the core into the cladding to determine the refractive index profile of the fiber. The fiber, immersed in a matching oil whose index of refraction is greater than that of the cladding, is passed through a small hole in an opaque disc. Part of the light focused into the fiber is guided while the rest appears outside of the fiber as a hollow cone. If all of the leaky modes, contained in the inner part of this cone are blocked by the disc, then the light passed varies linearly with the index of refraction of the fiber at the point at which the incident light is focused. Thus, by scanning the incident light across

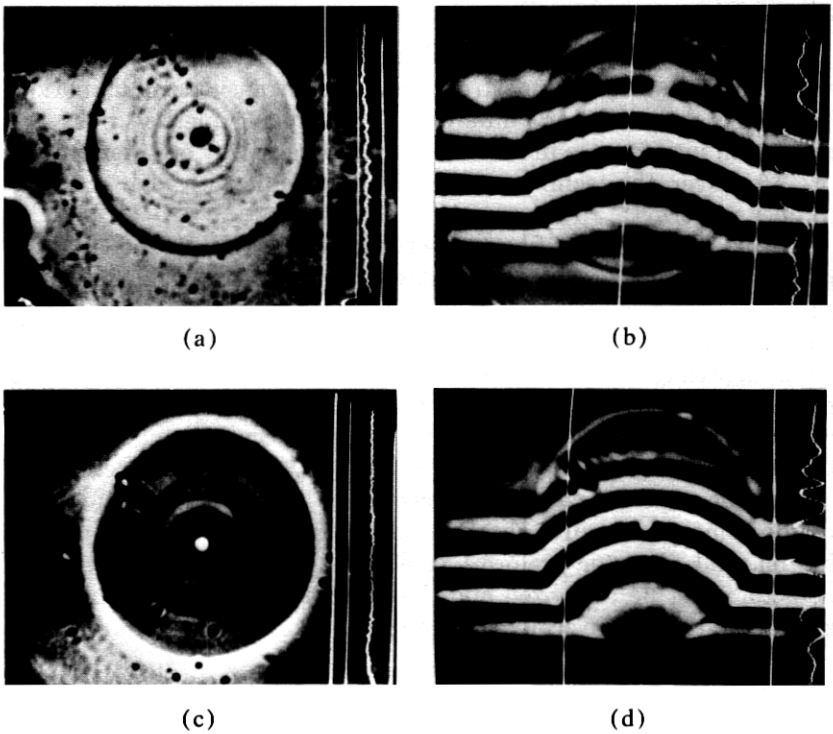

Fig. 4—Two fiber-SLAB samples observed by (a,c) ordinary microscopy, and by (b,d) interference microscopy.

the end of the fiber, the profile is obtained directly from the output of a detector that collects the light passing the disc.[16] This method, as will be seen in the profiles, has excellent spatial resolution and also possesses the ability to analyze noncircular cores. The precision of the index measurement is estimated in one recent embodiment[16] to be about 4×10^{-5}.

III. MEASUREMENT RESULTS

The fiber samples used in this study were specifically chosen to possess a variety of features, which would severely test the limits of the different profiling methods.

A SLAB sample of the first fiber is shown in Figs. 4a and 4b as observed with ordinary and interference microscopy, respectively. The fiber is seen to possess severe perturbation in layer structure throughout the core with marked variations especially near the center. The index profiles as obtained by the SLAB, FOCUS, and TRANS methods are shown in Fig. 5 by the solid, dotted, and dashed curves, respectively. The index and core radius values, which are in very good agreement,

are those obtained by each of the measurements and no scaling was employed. Generally the profile shapes are similar, with the TRANS profile exhibiting more detailed structure of the perturbations. Slight differences are accounted for by the assumption of circular symmetry in the FOCUS and TRANS cases and the lack of such an assumption for the SLAB.

A comparison of the RNF profile (solid curve) and the SLAB profile (broken curve) for this fiber is shown in Fig. 6. The SLAB, FOCUS, and TRANS profiles were all measured by the author at Bell Laboratories, Crawford Hill. The RNF profiles were provided by Jeff Saunders at Bell Laboratories, Atlanta.[16] The resolution of structure in the RNF profile is striking in comparison to the SLAB, which appears as a near average through the RNF results. The scale here and in subsequent profiles has been eliminated for clarity and ease of comparison. The RNF profile also shows a steeply rising region, and an index depression at the core-cladding interface, features not well resolved by the SLAB. The SLAB measurement is also not able to resolve the central depression due to its steep gradient.

A comparison of the RNF profile (solid curve) and the TRANS profile (broken curve) is shown in Fig. 7. The superior resolution of the TRANS

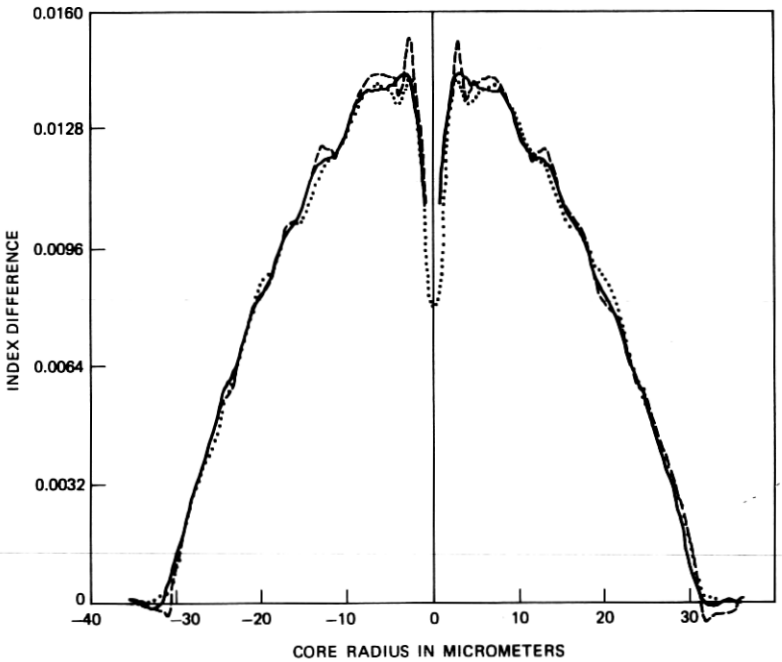

Fig. 5—Profiles of fiber shown in Figs. 4a and 4b (fiber no. 1) as obtained by SLAB (solid), FOCUS (dotted), and TRANS (broken) techniques.

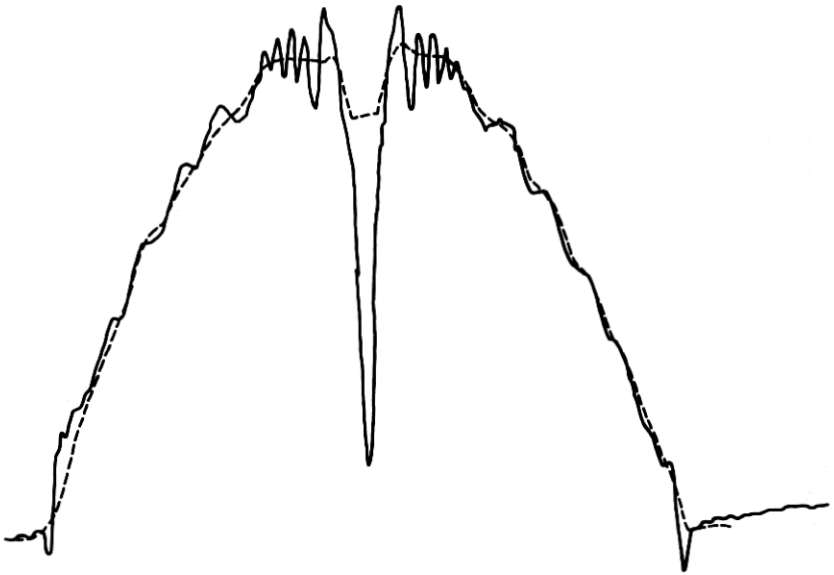

Fig. 6—Comparison of SLAB (broken) and RNF (solid) profiles for fiber no. 1.

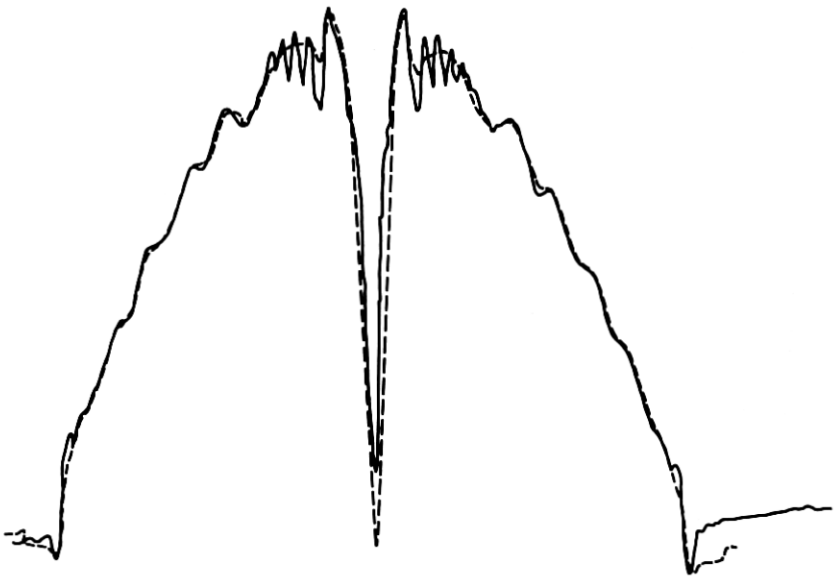

Fig. 7—Comparison of RNF (solid) and TRANS (broken) profiles for fiber no. 1.

measurement to that of the previously shown SLAB is clearly seen in that now the curves are practically identical, except for the region near the center where RNF shows greater detail.

The comparison of RNF (solid curve) and FOCUS (broken curve)

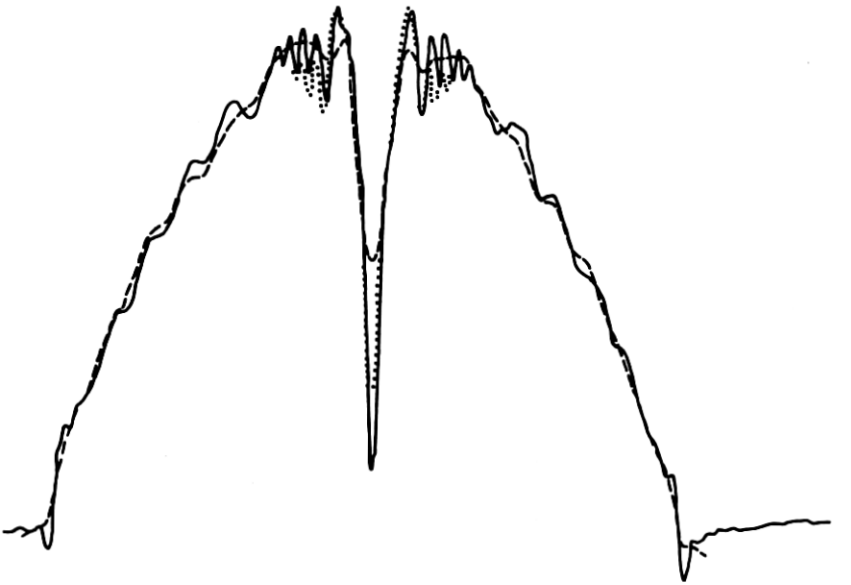

Fig. 8—Comparison of RNF (solid) and FOCUS (broken) profiles for fiber no. 1. The dotted curve is a portion of a focused profile obtained by focusing within the core.

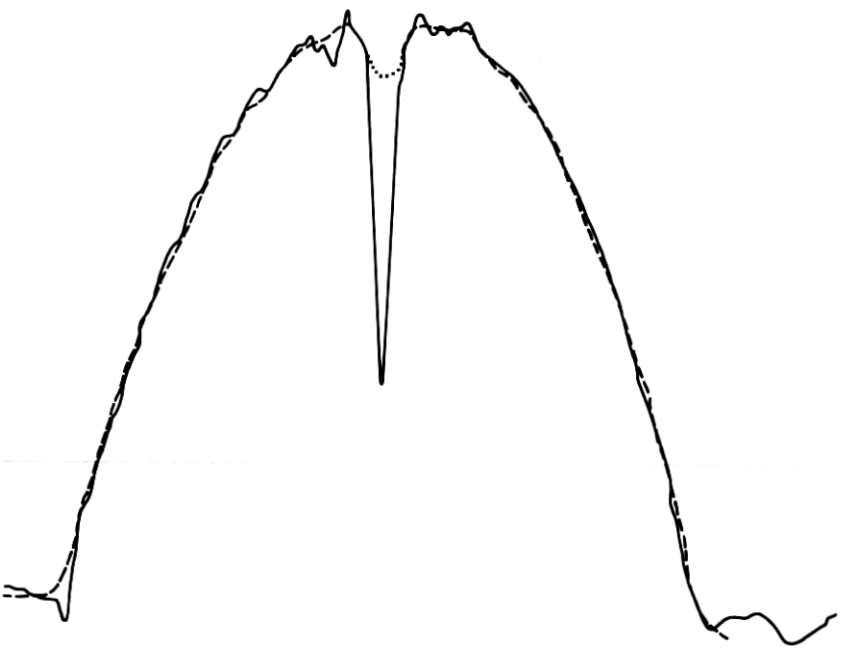

Fig. 9—Comparison of RNF (solid) and SLAB (broken) profiles for fiber shown in Figs. 4c and 4d (fiber no. 2).

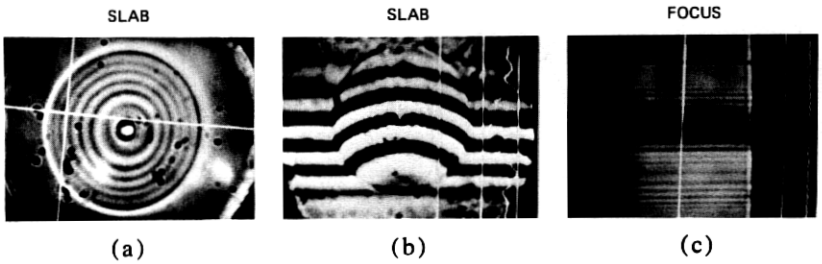

Fig. 10—Fiber no. 3 as observed by (a) ordinary microscopy, (b) slab interference microscopy, and (c) the focusing method.

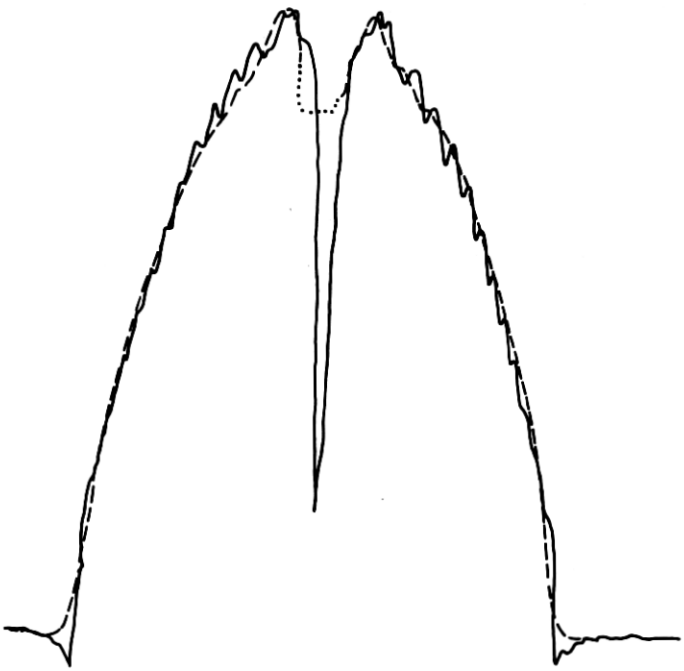

Fig. 11—Comparison of RNF (solid) and SLAB (broken) profiles for fiber no. 3.

shown in Fig. 8 is similar to the RNF versus SLAB results. A second FOCUS profile, a portion of which is shown by the dotted curve, was obtained by focusing within the core to obtain greater resolution. Indeed the resolution in this region is now comparable to RNF but the remainder of the profile (not shown) is distorted because of the violation of the focusing condition. Focusing within the core actually satisfies the focusing condition locally for those rapid variations that tend to focus the incident rays much more steeply than the remainder of the core.

A second SLAB sample with somewhat smaller index variations is

shown in Figs. 4c and 4d, again by ordinary and interference microscopy, respectively. A comparison of the RNF (solid curve) and SLAB (broken curve) profiles is presented in Fig. 9. Because of the smaller index fluctuations, the curves agree quite well but, again, the high resolution of RNF is apparent.

A third SLAB sample of a fiber fabricated with several (~10) discrete changes in dopant concentration as a function of core radius is shown in Figs. 10a and 10b by normal and interference microscopy, respectively. Figure 10c shows the whole fiber sample as observed by the focusing method.

A comparison of the RNF (solid curve) and SLAB (broken curve) profiles seen in Fig. 11 shows good agreement as far as the general profile shape is concerned, but the SLAB curve is, again, almost an average through the well-resolved layer structure of RNF. The FOCUS profile is similar to the SLAB, except when it is obtained by focusing within the core in which case specific local features can be brought out, at the expense of an overall distortion, with resolution comparable to RNF.

The TRANS profile of this fiber, shown by the broken curve in Fig. 12, is in excellent agreement with the RNF profile (solid curve). The resolution of the layers, the widths of which are somewhat larger than

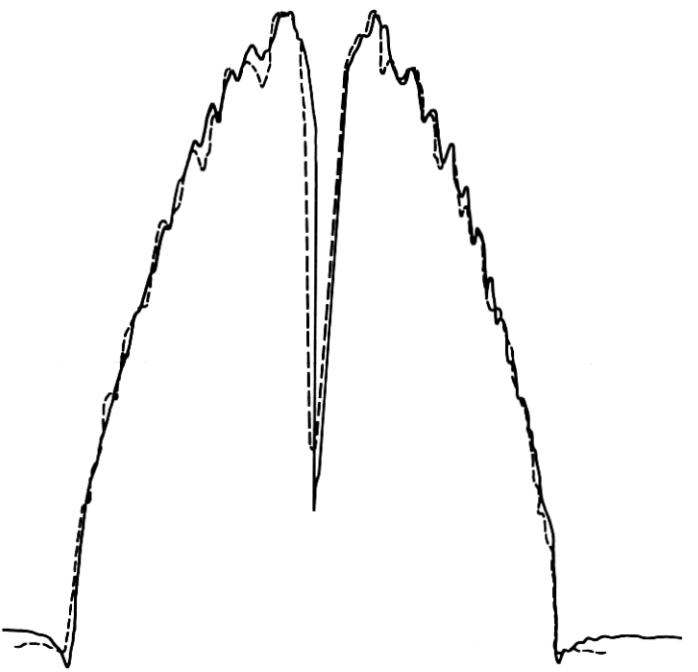

Fig. 12—Comparison of RNF (solid) and TRANS (broken) profiles for fiber no. 3. Note the comparable resolution.

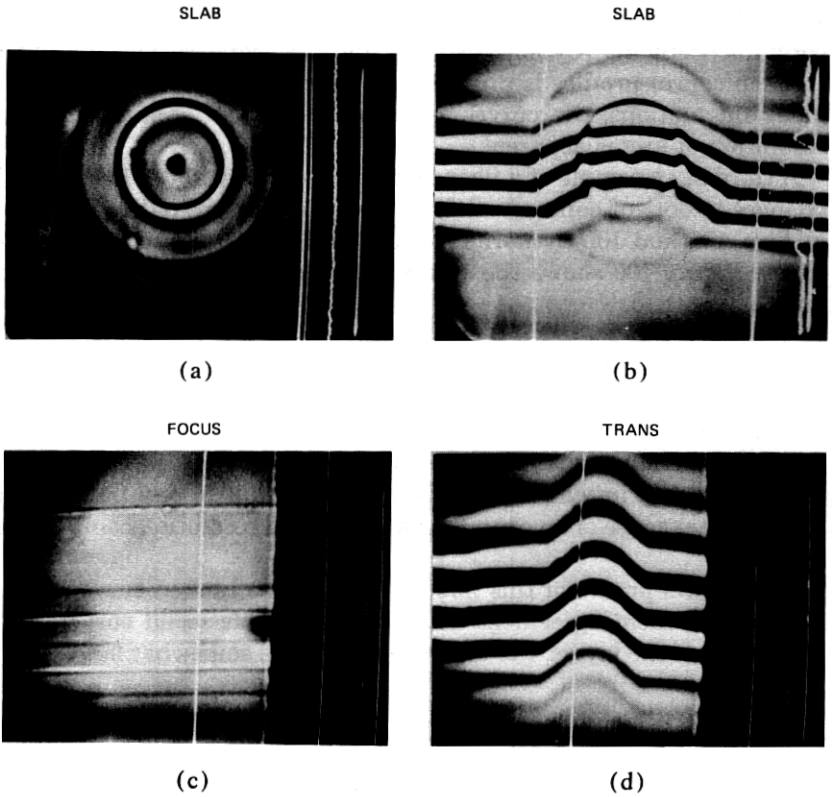

Fig. 13—Fiber no. 4, possessing a strong index perturbation, as observed by the various measurement methods.

in the first sample, is equally good. The index depression and steep rise in the index distribution are also the same in both.

A fourth sample having a major index perturbation at 50 percent of the radius is shown in Figs. 13a and 13d by ordinary microscopy, SLAB interferometry, focusing method, and transverse interferometry, respectively. The perturbation is clearly seen in each method of observation. A comparison of the SLAB (broken curve) and RNF profile (solid curve) is shown in Fig. 14. The profile shapes are similar but the index distortion is more prominent in the RNF measurement. The TRANS profile, shown as the broken curve in Fig. 15, on the other hand, shows the perturbation as clearly resolved as RNF (solid curve). The TRANS profile also displays the fine index variations, as does the RNF result, which lie closer to the center of the core. These fluctuations are absent in the SLAB and also in the FOCUS profiles both of which are very similar.

Finally, a fiber with a relatively perturbation-free index distribution

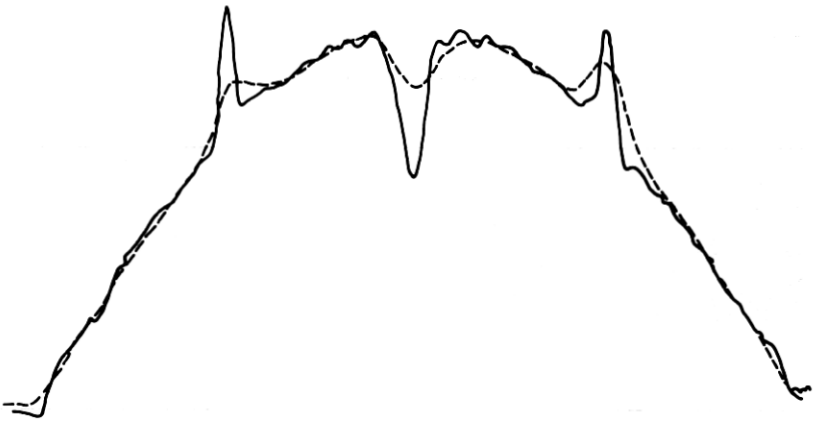

Fig. 14—Comparison of RNF (solid) and SLAB (broken) profiles of fiber no. 4.

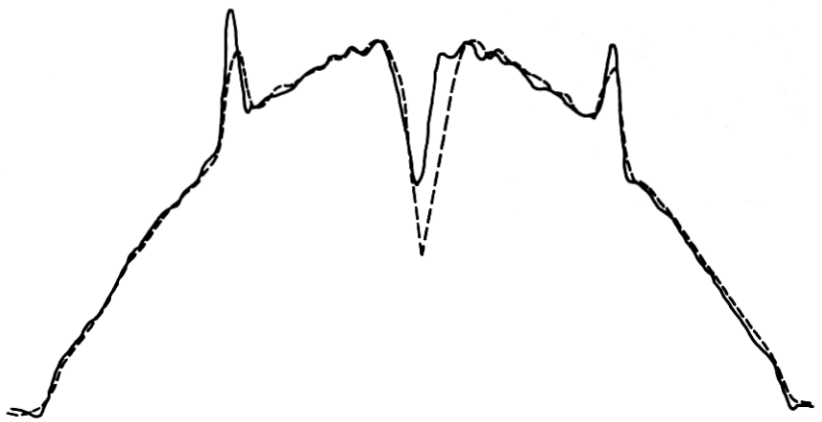

Fig. 15—Comparison of RNF (solid) and TRANS (broken) profiles for fiber no. 4.

was studied. The fiber as viewed by the SLAB, TRANS, and FOCUS techniques is shown in Fig. 16. To be noted in particular is the very uniform appearance (except for dirt specks) of all the samples indicating a lack of index distortions. The profiles obtained by the different methods, as might be imagined, are all very similar. The RNF (solid curve) and SLAB profiles (broken curve) are shown in Fig. 17 and the RNF (solid), FOCUS (dotted), and TRANS (broken) profiles are seen in Fig. 18. The only differences in the index distributions is a steep initial rise in the profile and some very slight ripple seen in the RNF result near the core center. This particular fiber also had a strong asymmetry in the index distribution near the center. This is not apparent in the FOCUS and TRANS results since they depend upon the assumption of circular symmetry.

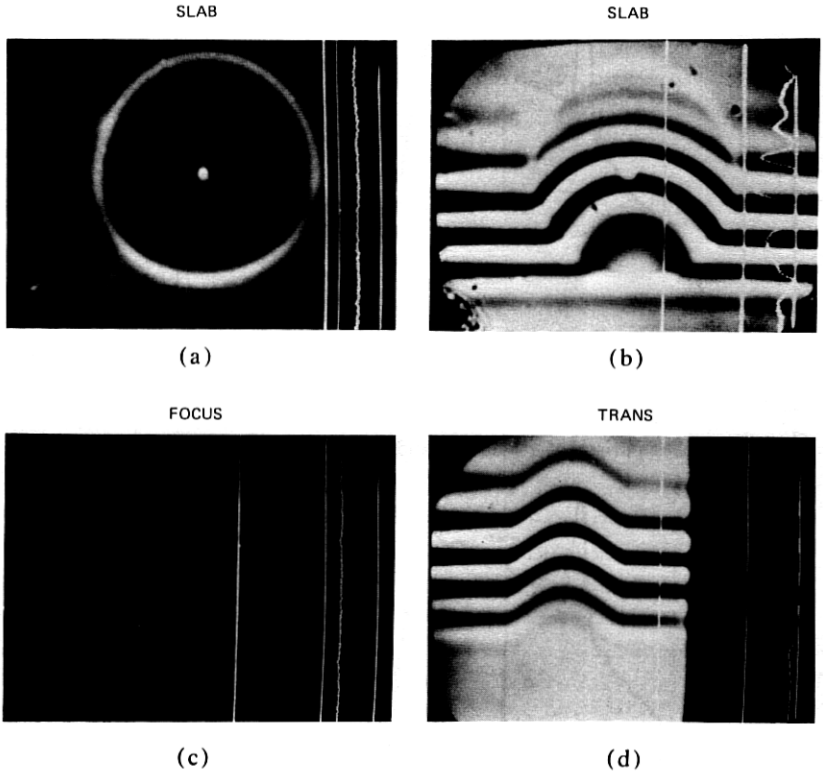

Fig. 16—Fiber no. 5 possessing a relatively perturbation-free profile as observed by the various measurement methods.

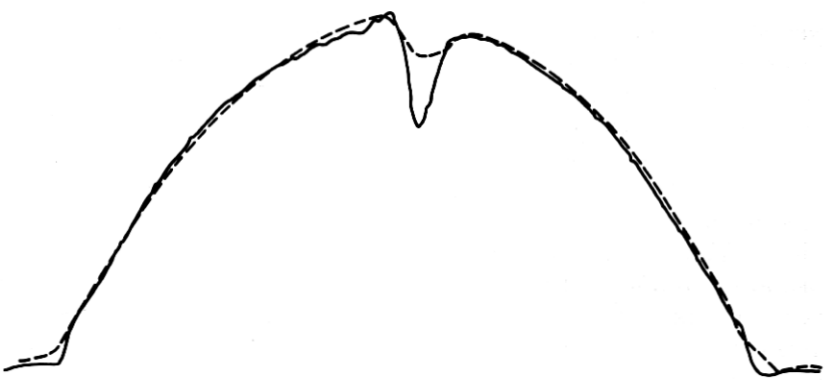

Fig. 17—Comparison of RNF (solid) and SLAB (broken) profile for fiber no. 5.

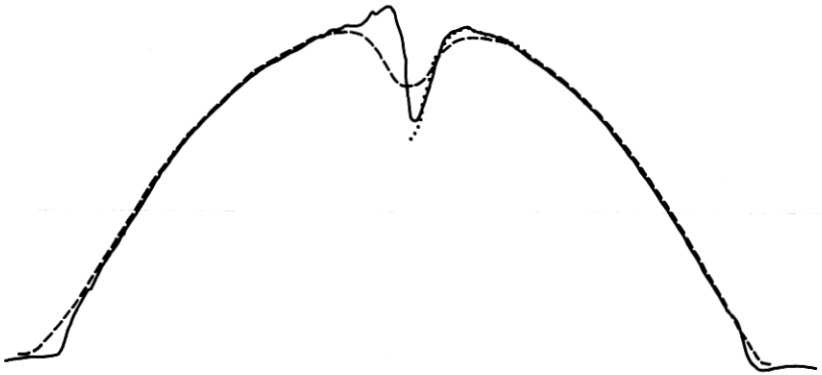

Fig. 18—Profiles of fiber no. 5 as measured by RNF (solid), FOCUS (dotted), and TRANS (broken) techniques.

An important question is the relationship of profiles measured in the fibers to the actual profile existing in the corresponding preforms. A knowledge of this relationship would shed additional light on the applicability of the various methods and give confidence that structural features observed in the fiber profiles are not measurement artifacts. Of particular interest is the steep initial rise in the index distribution of the last fiber as seen by RNF but not clearly defined with the other methods. Is this feature in the preform or not?

To answer this question the preform corresponding to the last sample was profiled by the two methods previously described, the focusing method as applied to preforms[3] and the ray-tracing technique as used at Western Electric's Engineering Research Center.[14]

The preform profiles are shown in Fig. 19; the solid curve is obtained by the ray-tracing technique and the broken curve by the focusing method. The profiles can barely be distinguished, except in the region near the center where the previously mentioned index perturbation makes the profile shape orientation dependent, and in the resolution of the finer deposition layers, which the ray-tracing method achieves by processing about ten times as many data points as the focusing method.

A comparison of the focused preform profile and the RNF fiber profile is shown in Fig. 20. Scaling of the radial coordinate, of course, was performed but not of the index values. The agreement of the profiles is excellent. It is seen that the initial steep rise which appears in the RNF profile is indeed present in the preform. It does, however, only appear as a single step in the RNF result, whereas in the preform it has a fine double-step structure. The chosen resolution of the focused preform profile is, thus, seen to correspond to the actual fiber profile. The greater detail included in the ray-tracing technique is absent even

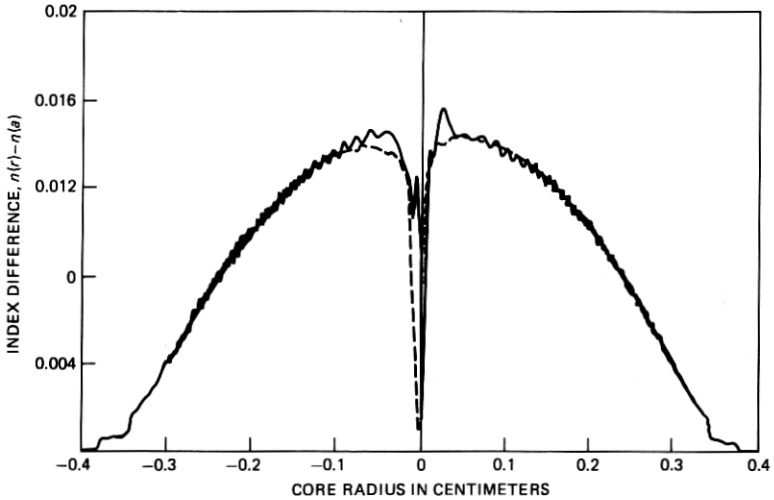

Fig. 19—Profiles of the preform stub from which fiber no. 5 was pulled as measured by the ray-tracing technique (solid curve) and the focusing method (broken). The two halves of each profile were obtained from measurements at two orientations.

from the RNF-profiled fiber, because of its small-scale structure. In general, a very high degree of correspondence between fiber and preform profiles exists.

The various fiber profiles were further compared by taking the rms deviation of their differences as a function of radial position. This is the severest possible comparison in that absolute point-by-point values are looked at. Thus, a slight shift of a feature could result in a sizable difference. A second less restrictive comparison was also made by computing the best-fit g values to the various profiles. This emphasizes the profile shape at the expense of the location and existence of small perturbations.

It was found that the various profiling methods give just about identical results for relatively smooth profiles. The rms deviations of the profiles of the last fiber (shown in Figs. 16–20), were all less than one percent, excluding the index depression in the center. The central depression gives rise to a few percent difference on its own because of the different ways it is resolved by the various methods. The best fit g curves were all within 0.05 of each other. The RNF profile has a g value of 2.024 and that of the preform (as measured by the focusing method) a value of 1.990, a difference of less than 0.035.

As expected, the rms differences between the profiles increase for those possessing rapid variations. These differences for the first four fiber samples shown amounted to three to five percent, again excluding the index depression. The g values of the respective profiles were all

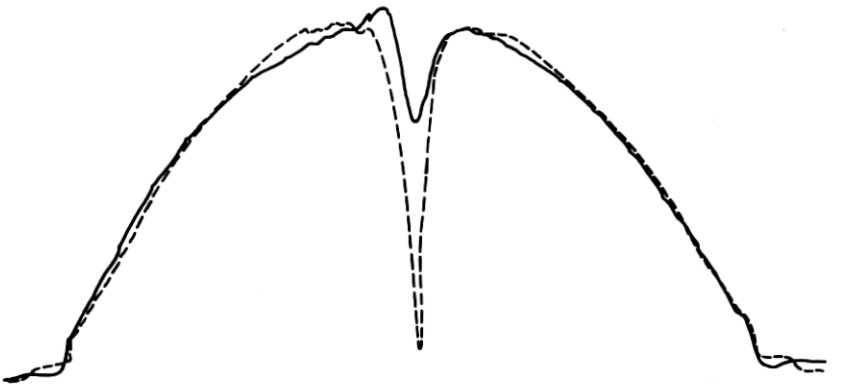

Fig. 20—Comparison of preform profile (broken) and corresponding RNF fiber profile (solid) for fiber no. 5.

within a few percent, as would be expected from the similarities of the curves.

We conclude then, that as long as the profile is smooth all of the measurement methods are equivalent. For profiles containing rapid perturbations, the RNF and TRANS methods are about comparable with the former doing better in resolving very rapid variations. The RNF method also has the advantage of not requiring an interference microscope nor elaborate computer processing of the data. On the other hand, it does require a separate calibration procedure and reasonable care with cleanliness of the optics.

The fact that the rms deviations are less than one percent and the best-fit g values are within 0.05 for relatively perturbation free profiles lends confidence to the ability to make valid bandwidth predictions for current fibers of this type based on the various measured profiles.[17] Deviations of this magnitude, while reducing the bandwidth by about one order of magnitude, still result in bandwidths close to 1 GHz. As profiles get even smoother these deviations will presumably decrease and allow for even better predictions. Meanwhile, improvements in the accuracy of the profiling methods themselves, can also serve to reduce these interprofile deviations and lead to even better agreement. An improvement in accuracy of about a factor of 5 is required to meaningfully measure deviations of the ideal profile. On the other hand, one then enters the realm of theoretical uncertainty as to what the ideal ideally is. The current state-of-the-art of index measurements should then be able to go a long way in providing the feedback necessary to improve current profiles before their limitations are indeed felt.

While we have presented four current profiling techniques, there are, of course, other existing methods each subject in use to their own

set of trade-offs. New methods both for fibers and preforms are reported regularly and undoubtedly as they prove their value will find use in the important task of index profiling.

IV. ACKNOWLEDGMENTS

The author thanks J. Saunders for providing the RNF profiles, L. Watkins for supplying the ray-tracing profile of the preform, and D. Marcuse for computational analysis.

APPENDIX

Implementation of Profile Measurement Methods

Preform diagnostigrams

Preform diagnostigrams provide a sensitive, nondestructive, and noncontacting means of obtaining structural information. This information includes a measurement of core size and core eccentricity, core cladding interface structure, individual deposition layer structure and variations, imperfections within the core and the cladding, and the presence of an axial refractive-index depression.

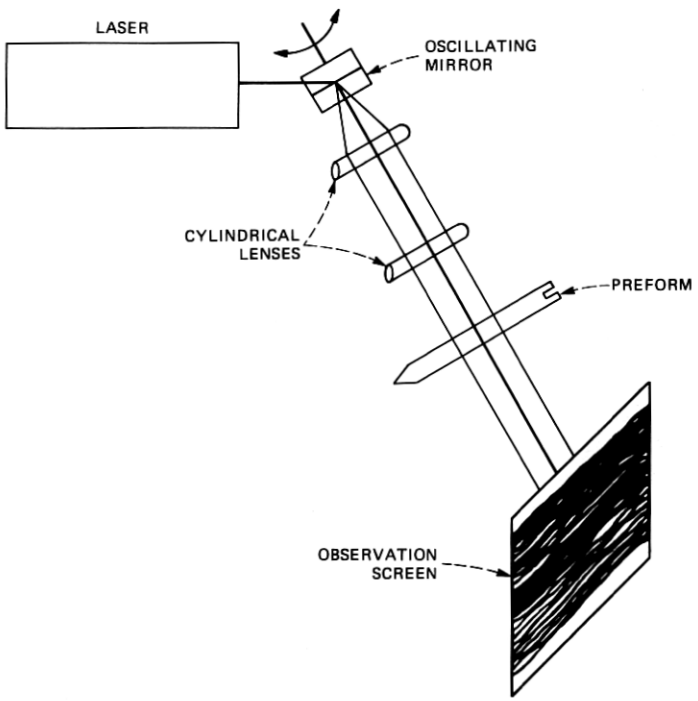

Fig. 21—Arrangement to produce preform diagnostigrams.

A diagnostigram is produced by the arrangement shown in Fig. 21. Light from a He-Ne laser is incident upon an oscillating mirror that serves to transform it into a line. The line of light is expanded and collimated by two cylindrical lenses and traverses the preform. The beam is about equal in width to the diameter of the preform, and its length can be varied as desired by adjusting the amplitude of the oscillating mirror. Typically a length of 15 cm is used. An arrangement of cylindrical lenses replacing the oscillating mirror can also be utilized. The light traversing the preform is then incident upon either an observation screen or photographic film.

The pattern, as shown in Fig. 1a (of the text), consists of bright and dark lines. The width of the bright lines represents the actual geometric width of discontinuous index steps in the core, while the width of the dark lines represents the amount Δn of refractive-index discontinuity. The discontinuities arise during the deposition process and represent distinct deposition layers. There exists a one-to-one correspondence between the observed lines and the deposited layers. Further details can be found in Ref. 2.

Slab and transverse interferometry

In slab interferometry the fiber sample is placed in one arm of the interference microscope and a homogeneous reference SLAB with refractive index n_2 is placed in the reference arm (Fig. 2a). An arrangement of practical implementation is shown in Fig. 22. Figure 23 displays the fringe shifts observed in a graded-index sample, the shift S of a fringe depending on its position in the fiber core, $S = S(r)$. The difference between the refractive indices of core and cladding can be expressed in terms of this fringe shift $S(r)$, the uniform fringe spacing in the cladding D, the vacuum wavelength of light λ, and the SLAB thickness t as

$$n(r) - n_2 = \frac{\lambda S(r)}{Dt}. \tag{1}$$

To measure the fringe shift a video camera looks into the interference microscope and sends its electrical output signal to a video digitizer. The 8-bit digitizer is computer controlled and addresses specific, preselected points in the video field. A video monitor and a plotter for recording the processed information—the index profile, is also included. The computer directs the vertical sample line seen in Fig. 23 to collect information on either side of the core (along lines A-B, and C-D), which is then used to determine the fringe spacing and to compensate for a tilt of the entire fringe pattern. The computer then advances the sample line in small increments, moving it through the core region, measuring the displacement of the fringe that goes through

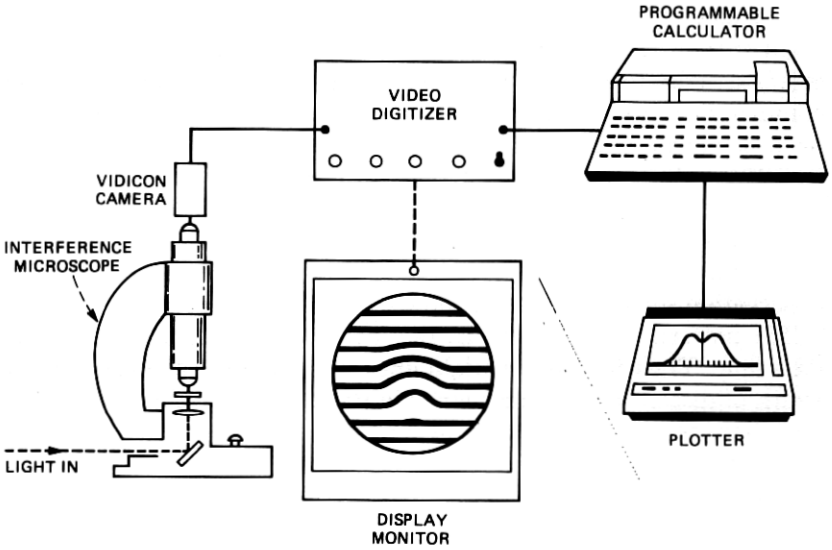

Fig. 22—Arrangement for automatic refractive index profiling of SLAB samples.

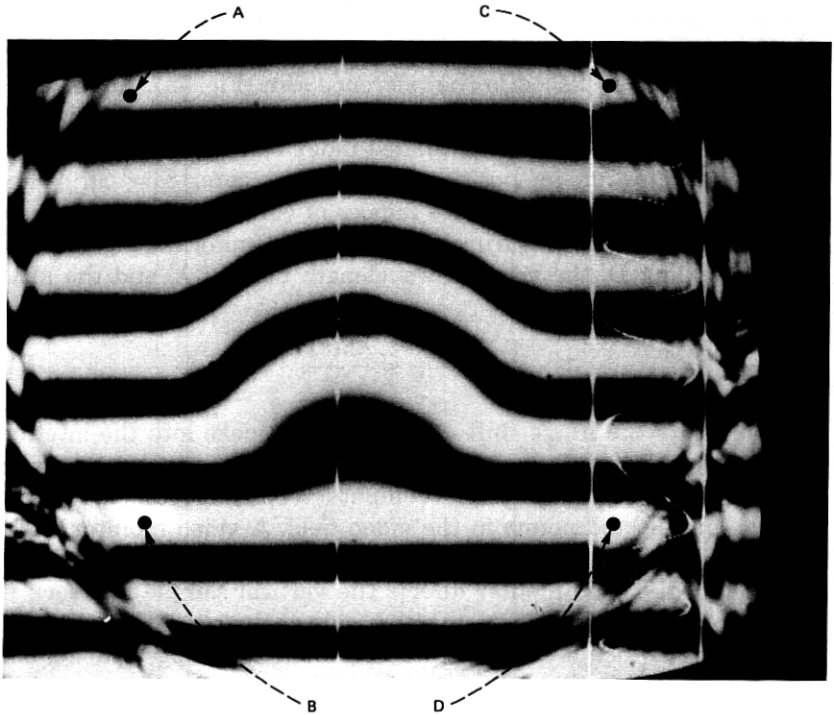

Fig. 23—Fringes observed in a graded-index SLAB sample.

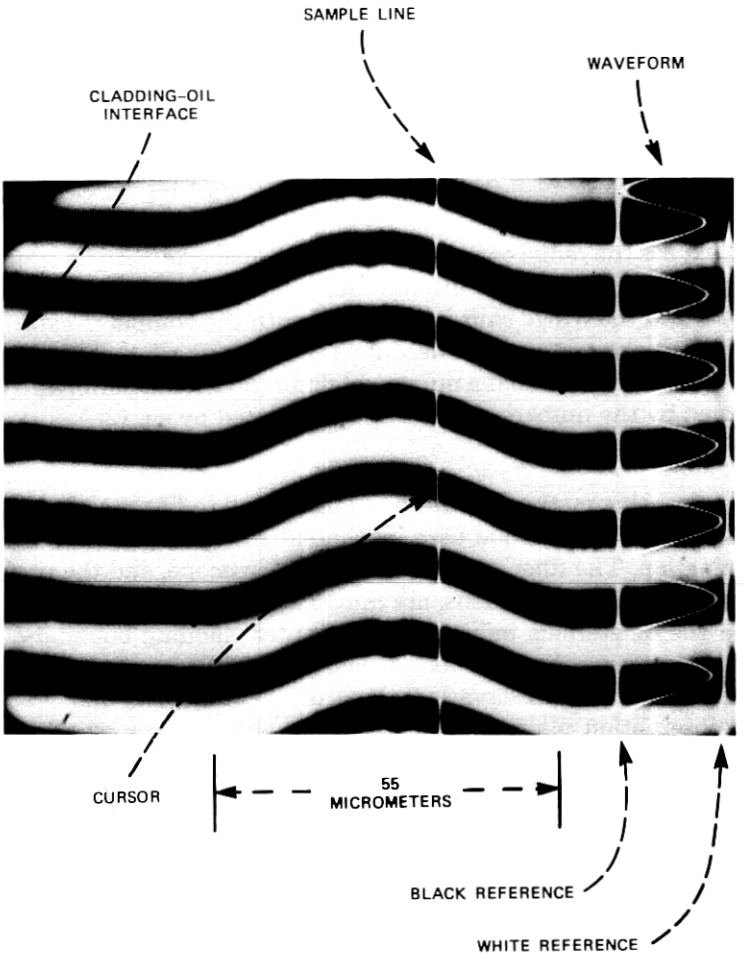

Fig. 24—Fringes observed in a graded index whole fiber sample observed transversely.

the core center. The computer determines the fringe positions by counting and searching for the minimum light level whose location it pinpoints by least mean square fitting of a parabola using a number of points in the vicinity of the minimum.

The fringe displacement is recorded as a function of the radial coordinate r measured from the core center and the resulting function $S(r)$ is used to compute $n(r) - n_2$ according to eq. (1). The index distribution is then sent to the plotter.

In transverse interferometry the fiber, after being stripped of any jacket, is again placed in one arm of the interference microscope (Fig. 2b in text). The fiber is covered with a drop of matching oil into which the microscope objective is dipped. The reference branch contains only

a drop of matching oil. Each light ray incident upon the sample now passes through regions of varying refractive index and the total path length must be expressed as an integral. The refractive index difference between core and cladding is given by

$$n(r) - n_2 = \frac{\lambda}{\pi D} \int_r^\infty \left| \frac{dS(\rho)}{d\rho} \right| \frac{d\rho}{\sqrt{\rho^2 - r^2}} \tag{2}$$

in which ρ is the radial coordinate and rotational symmetry is assumed.

The output field of the interference microscope now appears as in Fig. 24, and the fringe shift is measured with the computer-controlled video digitizer system just described. Processing of the fringe shift information requires that a numerical differentiation is performed first, followed by the numerical integration indicated by eq. (2).

The focusing method

The focusing method is shown in application to fibers and preforms in Fig. 25. The technique uses incoherent filtered light in transverse illumination. The fiber, observed with a microscope, and the preform, observed with a camera lens, are immersed in index matching fluid to avoid the deleterious influence of the outer cladding boundary. The core, acting as a cylindrical lens, focuses the light whose power density distribution in the observation plane is detected by a video camera. The observation plane is defined by the object plane on which the camera is focused. This plane must not be inside the fiber core, and it must not be placed so far away that rays have already crossed over after leaving the core. Good results are obtained when the observation plane is placed just outside of the core.

The image of a preform seen by the camera is shown in Fig. 1b of the text. A monitor display of a fiber is shown in Fig. 26.

The refractive index distribution is obtained by solving the integral equation

$$n(r) - n_2 = \frac{n_2}{\pi L} \int_r^\infty \frac{t - y(t)}{\sqrt{t^2 - r^2}}\, dt. \tag{3}$$

The various parameters are defined in Fig. 3a of the text.

The function $y(t)$ is obtained from a measurement of the light power density distribution in the observation plane. This distribution is collected along the sample line and digitized under computer control as described previously. The computer also solves the integral equation and plots the resultant index profile.

Refracted near-field method

In this technique[15] (shown in Fig. 3b of the text) a light beam is focused on a spot at a distance r from the fiber axis with a convergence

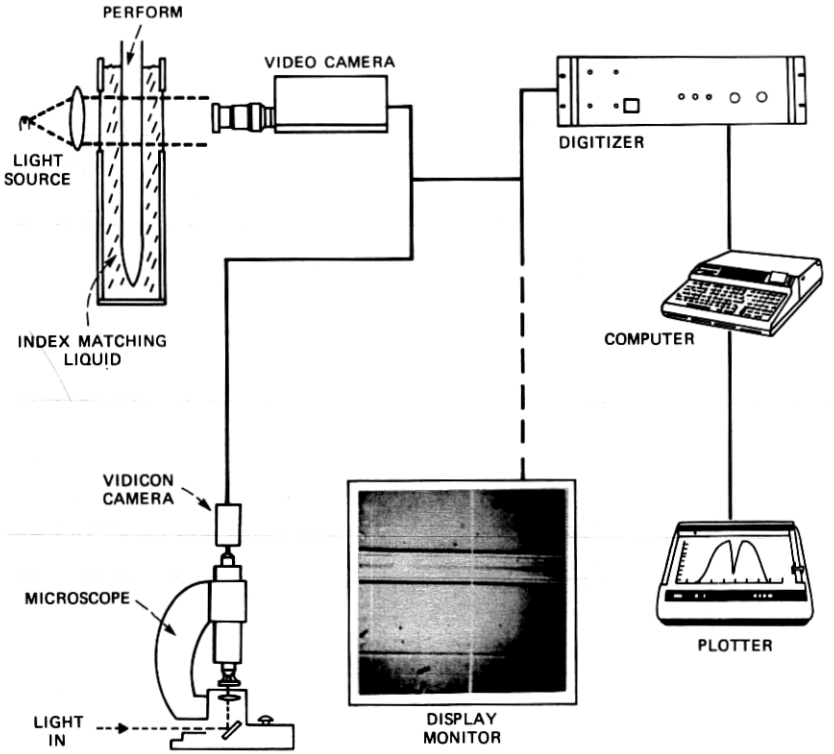

Fig. 25—Arrangement for automatic refractive index profiling of fibers and preforms by the focusing method.

angle that is larger than the acceptance angle of the fiber core. The light escaping from the core is partly contributed by power leakage from leaky modes. This part of the radiated power is blocked by a circular aperture which prevents light leaving below a minimum angle $\theta''_{\min}$ from reaching the detector. The refractive index difference between the core and cladding, which is obtained from the light passed by the aperture, is given by

$$n(r) - n_2 = n_2 \cos \theta''_{\min} [\cos''_{\min} - \cos \theta''_{\max}] \frac{P(a) - P(r)}{P(a)}. \qquad (4)$$

In this expression θ'' refers to the input angle, $P(r)$ is the light power reaching the detector, as a function of the position of the input beam and $P(a)$ is obtained from the $P(r)$ curve as the light power detected when the input beam is focused into the cladding.

The experimental apparatus used in the implementation of this method by J. Saunders is shown in Fig. 27.[16] Light from a 5-mW He-Ne laser passes through a quarter wave plate and is focused onto a 50-

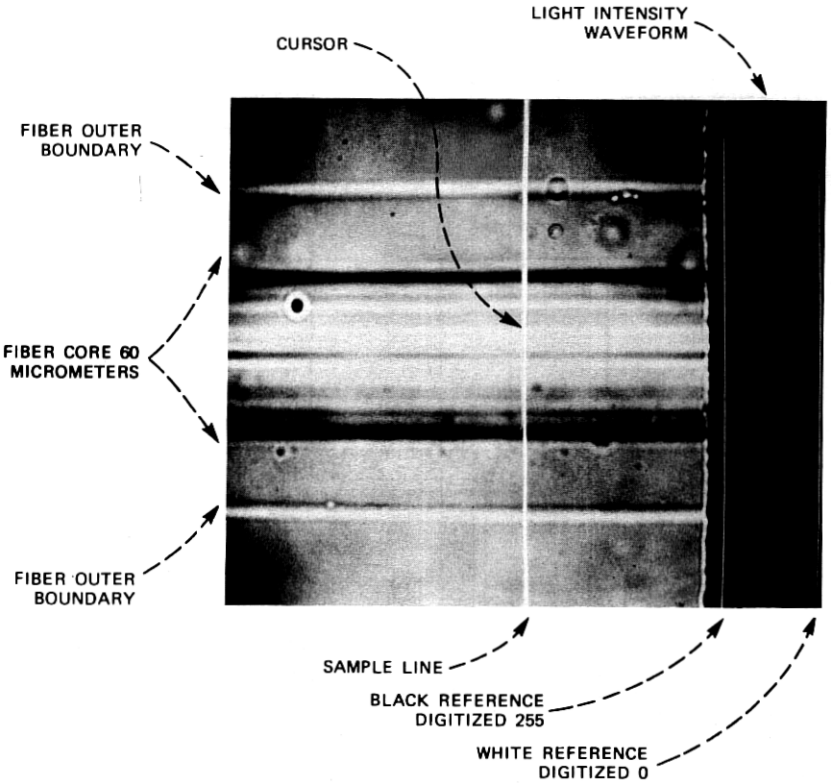

Fig. 26—Graded-index fiber as observed by the focusing method.

μm pinhole. The light from the pinhole is then focused by a 20x microscope objective onto the end face of the fiber which is held in a moveable cell containing index immersion liquid.

The disc that blocks the leaky rays is 1.3 cm in diameter and is supported by means of three fibers. The light passing the disc is directed by lenses to a large area detector whose output provides the profile. The microscope and TV camera provide a magnified view of the fiber core for alignment and monitoring purposes.

Ray-tracing method

The practical implementation of this method by L. S. Watkins, is shown in Fig. 28.[14] A narrow beam from a He-Ne laser is reflected off a rotatable mirror and is focused by a lens through the index-matched preform. Rotating the mirror moves the ~20 μm beam across the preform.

The deflected beam is collected by a lens and focused onto a linear

position sensor at its back focal plane. The output of the sensor is analyzed to give a voltage proportional to the deflection angle, which is then computer-processed in a similar manner to the focusing method to give the profile.

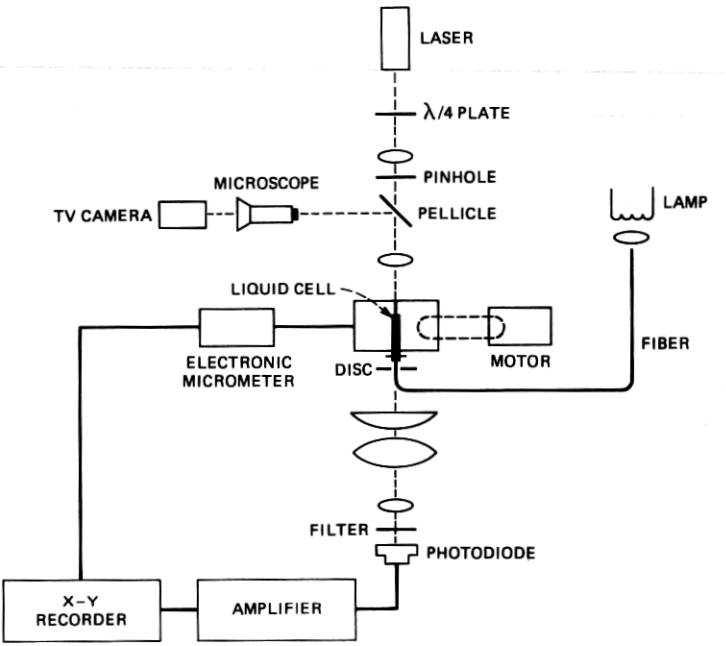

Fig. 27—Experimental apparatus for implementation of the RNF method.

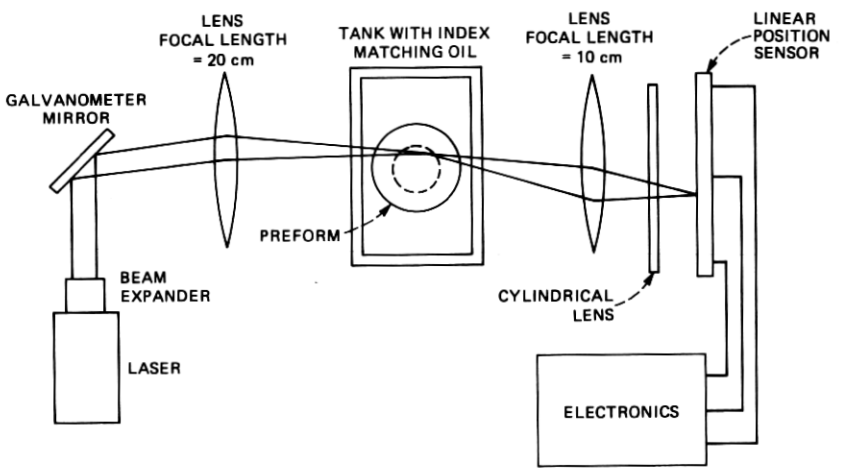

Fig. 28—Arrangement for profiling of preforms by the ray tracing method.

REFERENCES

1. J. B. MacChesney, P. B. O'Connor, and H. M. Presby, "A New Technique for the Preparation of Low Loss and Graded-Index Optical Fibers," Proc. IEEE, *62* (September 1974), pp. 1280–1.
2. H. M. Presby and D. Marcuse, "Optical Fiber Preform Diagnostics," Appl. Opt., *18* (1979), pp. 23–30.
3. H. M. Presby and D. Marcuse, "Preform Index Profiling (PIP)," Appl. Opt., *18* (March 1979), 671–77.
4. H. M. Presby, et al., "Material Structure of Germanium-Doped Optical Fibers and Preforms," B.S.T.J., *54,* No. 10 (December 1975), pp. 1681–92.
5. S. Suzuki et al., "Transmission Characteristics of Graded-Index Fiber," Technical Digest, 1977 Int. Conf. Integrated Optics and Optical Fiber Commun. (IOOC) (1977) p. 459.
6. D. Marcuse and H. M. Presby, "Effects of Profile Deformations on Fiber Bandwidth," Appl. Opt., *18* (1979) p. 3758.
7. C. A. Burrus and R. D. Standley, "Viewing Refractive-Index Profiles and Small-Scale Inhomogeneities in Glass Optical Fibers: Some Techniques," Appl. Opt., *13* (1974) p. 2365.
8. J. Stone and R. M. Derosier, "Elimination of Errors Due to Sample Polishing in Refractive-Index Profile Measurements by Interferometry," Rev. Sci. Instrum., *47* (1976), p. 885.
9. H. M. Presby and H. W. Astle, "Optical Fiber Index Profiling by Video Analysis of Interference Fringes," Rev. Sci. Instrum., *49* (1978), pp. 339–44.
10. E. Ingelstam and I. P. Johansson, "Correction Due to Aperture in Transmission Interference Microscopes," J. Sci. Instrum., *35* (1958), p. 15.
11. H. M. Presby, et al., "Rapid Automatic Index Profiling of Whole-Fiber Samples: Part II," B.S.T.J., *58,* No. 4 (April 1979), pp. 883–902.
12. D. Marcuse, "Refractive Index Determination by the Focusing Method," Appl. Opt. *18* (1979), pp. 9–13.
13. D. Marcuse and H. M. Presby, "Focusing Method for Nondestructive Measurement of Optical Fiber Index Profiles," Appl. Opt., *18* (1979), pp. 14–22.
14. L. S. Watkins, "Laser Beam Refraction Transversely Through a Graded-Index Preform to Determine Refractive Index Ratio and Gradient Profile," Appl. Opt., *18* (1979), 2214–22.
15. W. J. Stewart, "A New Technique for Measuring the Refractive Index of Graded Optical Fibers," Technical Digest, 1977 Int. Conf. Integrated Optics and Optical Fiber Commun. (IOOC) Tokyo, Japan, July 18–20, 1977.
16. M. J. Saunders, "Optical Fiber Profiles Using the Refracted Near Field Technique: A Comparison With Interferometry," Technical Digest Supplement, Symp. Optical Fiber Measurements, Boulder, Colorado, October 28–29, 1980.
17. H. M. Presby, D. Marcuse, and L. G. Cohen, "Calculation of Bandwidth from Index Profiles of Optical Fibers. Part 2: Experiment," Appl. Opt., *18* (1979), pp. 3249–55.